HHS Public Access

Author manuscript

Dev Biol. Author manuscript; available in PMC 2021 October 01.

Published in final edited form as:

Dev Biol. 2020 October 01; 466(1-2): 47–58. doi:10.1016/j.ydbio.2020.08.003.

Drainage of amniotic fluid delays vocal fold separation and induces load-related vocal fold mucosa remodeling

Vlasta Lungova[1], **Kate V. Griffin**[1], **Tadeas Lunga**[1], **Susan L. Thibeault**[1]

[1]Department of Surgery, UW Madison, 1111 Highland Ave, WIMR, Madison WI, 53705 USA

Abstract

In the present study, we investigated the role of mechanical load as generated by amniotic fluid in the vocal fold embryogenesis. *In utero*, amniotic fluid flows through the laryngeal inlet down into the lungs during fetal breathing and swallowing. In a mouse model, the onset of fetal breathing coincides with epithelial lamina recanalization. The epithelial lamina is a temporal structure that is formed during early stages of the larynx development and is gradually resorbed whereby joining the upper and lower airways. Here, we show that a temporary decrease in mechanical load secondary to drainage of amniotic fluid and subsequent flow restoration, impaired timing of epithelial lamina disintegration. Moreover, re-accumulation of fluid in the laryngeal region led to VF tissue deformation triggering remodeling of the epithelium and pressure generated changes in the elastic properties of the lamina propria, as measured by atomic force microscopy. We further show that load-related structural changes were likely mediated by Piezo 1 –Yap signaling pathway in the vocal fold epithelium. Understanding the relationship between the mechanical and biological parameters in the larynx is key to gaining insights into pathogenesis of congenital laryngeal disorders as well as mechanisms of vocal fold tissue remodeling in response to mechanotransduction.

Keywords

development; mechanical forces; epithelial lamina recanalization; tissue remodeling

Introduction

Mechanical forces provide essential epigenetic clues that drive developmental processes, such as cardiogenesis and valvulogenesis (1,2) and the development of lungs, tendons and muscles (3,4). These extracellular forces are converted into intracellular signals that can trigger various cellular responses such as cell division, survival, migration and

Author contribution

V.L. and S.L.T. designed research; V.L. performed IF staining for selected genes and markers of epithelial and mesenchymal cells and qPCR analyses. K. V. G. performed vibratome sectioning, elastic modulus measurements and statistical analyses. T. L. performed surgeries on mice, hematoxylin-eosin staining and isolated RNA for the q PCR analysis. V.L. and S.L.T. wrote the paper. All authors approved the final manuscript.

differentiation (5–8). For example, hemodynamic forces generated by blood flow are transformed by endocardial cells to paracrine signals that cause extracellular matrix remodeling and errors in the transmission of such signals may result in congenital valve diseases (1). Accordingly, changes in amniotic fluid pressure in fetal lung epithelium can lead to abnormal lung development and defects that persist throughout life (3). Similar to these mechanically active organs, the larynx and vocal folds (VF) are also exposed to mechanical pressure during VF embryogenesis. *In utero*, mechanical load is generated by amniotic fluid that flows through the laryngeal inlet down into the lungs during fetal breathing and swallowing. The role of this mechanical load on development of the larynx and VF has not been investigated to date.

Development of the larynx commences around embryonic (E) day 10.5 in mice and week 4 in humans, when lateral walls of the primitive laryngopharynx, VF primordia, start to grow into the center of the lumen and fuse together to create the epithelial lamina (EL) (9–12). The EL is a temporal structure, which disintegrates between E13.5 and E18.5 in mice and weeks 7 and 10 (up to week 12) in humans. EL establishment is essential for 1) formation of the tracheoesophageal septum, 2) establishment of VF epithelial basal progenitors and 3) further differentiation of mesenchymal structures into connective tissue of the lamina propria (LP), laryngeal cartilages and muscles, which complete their development prior to VF separation (13). Disruption of proper differentiation of VF epithelial and/or mesenchymal cells can lead to failure of EL recanalization, causing congenital laryngeal webs (13). Laryngeal webs can be life-threatening at birth and cause problems with voicing and breathing across the life span (14–16).

Regardless of the importance of EL recanalization little is known about how the process is regulated. Genetic studies have shown that signals mediated by retinoic acid and beta Catenin are involved in the EL recanalization(13,16,17). In the present study, we investigated the role of mechanical forces in this process. Based on the previous investigations, the early stages of the EL recanalization coincide with the onset of the fetal breathing in mice (18). Inhaled amniotic fluid thus flows through the laryngeal inlet down into the lungs (3) and exerts pressure on the laryngeal cavities that gradually expand and open the laryngotracheal tube. Here, we show that a decrease in mechanical load due to drainage of amniotic fluid and consequent flow delayed EL disintegration. Moreover, re-accumulation of fluid in the laryngeal region applied mechanical stress on the epithelial walls, which led to VF tissue deformation that triggered intense remodeling of the epithelium and pressure generated changes in elastic properties of the lamina propria (LP), as measured by atomic force microscopy (AFM). We further show that load-related structural changes in the epithelium and LP were likely mediated by Piezo 1 – Yap signaling pathway in the VF epithelium.

Materials and Methods

Mouse mating and tissue collection

Wild-type FVB males and females were mated, and noon of the day when vaginal plugs were found was designated as E 0.5. Pregnant females at day 15.5 gestation underwent surgery under isoflurane anesthesia (Fig.1). The peritoneum was opened, and embryos were

removed. One third of the total number of embryos underwent a puncture of the amniotic sac with a 25G needle. Remaining embryos were left as controls to prevent spontaneous abortion or preterm labor. After the perforation, embryos were returned to their initial position. The peritoneal cavity was flushed with saline and closed with sutures, the skin was closed with clips. Pregnant females were then sacrificed at E16.5, E17.5, and E18.5 [24, 48 and 72 hours (h), post-surgery (PS)] following regulations of protocols approved by the University of Wisconsin Animal Care and Use Committee. Control and drained embryos were removed from the amniotic sacs, mouse larynges were dissected out and used for immunohistochemistry, RNA isolation for quantitative Polymerase Chain Reaction (qPCR) and elastic modulus measurements to examine viscoelastic properties of the VF LP.

Immunohistochemistry

Dissected larynges from control and drained murine embryos at each time point (24, 48 and 72h PS) were fixed in 4% paraformaldehyde in phosphobuffered saline (PBS) at 4°C/ overnight, dehydrated in a gradient series of ethanol, treated with xylene and embedded in paraffin. Paraffin blocks were cut into serial coronal sections (5 μm), dewaxed and rehydrated. Hematoxylin-eosin staining was performed to assess the tissue morphology. Remaining sections were stained using a standard immunofluorescent protocol (IF) protocol (10). Antigen retrieval was performed by heating sections in sodium citrate pH = 6 at 80°C water bath for two hours followed by treatment with 0.5% Triton for 20 min/RT. Primary antibodies used are: goat anti-rabbit NKX2.1 (Abcam, Cambridge, CA, USA) diluted to 1:200, goat anti-mouse SOX2 (Thermo fisher Scientific, Waltham, MA, USA) diluted to 1:100, goat anti-rabbit Yap (Cell Signaling, Danvers, MA, USA) diluted to 1:100, goat anti-mouse p63 diluted to 1:100 (Santa Cruz Biotechnology, Dallas, TX, USA), goat anti-rabbit Cytokeratin K8 diluted to 1:250 (LS Bio, Seattle, WA, USA), goat anti-mouse Collagen1 (Abcam, Cambridge, CA, USA) and goat anti-rabbit Piezo1 (Novus Biological; Littleton, CO, USA) diluted to 1:100. They were applied overnight at 4°C degrees. Secondary antibodies used are: Cy3-cojugated goat anti-mouse at the dilution 1:200 (Jackson ImmunoResearch; West Grove, PA, USA), and Alexa Fluor TM 594 goat anti-rabbit (Invitrogen, Carlsbad, CA, USA) at the dilution 1:500. They were applied 1h and 30 min at room temperature (RT). Slides were mounted using Vectashield with DAPI (Vector Laboratories; Peterborough, UK). Images were taken with a Nikon Eclipse E600 with a camera Olympus DP71, images were adjusted for brightness using the installed DP 71 software, Olympus Corporation. Figure panels were created using MS PowerPoint 2010.

RNA isolation and quantitative Polymerase Chain Reaction

Dissected larynges from control and drained murine embryos at each time point (24h, 48h and 72h PS) were used for RNA isolation using ReliaPrep™ RNACell Miniprep System (Promega, Madison, WI, USA) following manufacturer's protocol. For each control and drained group, three larynges were pooled together to maximize total RNA yield (n=3 for one biological replicate). One thousand ng of RNA was then reverse transcribed to cDNA using reverse transcription reagents (Go Script, Promega, Madison, WI, USA) per manufacturer's protocol. Consequently, expression levels of selected genes were analyzed with qPCR. Total volume of 0.4μl of cDNA was used per 20μl real time qPCR reaction using Power Up Sybr Green Master Mix (Applied Biosystem, Foster City, CA, USA) and run for

40 cycles in triplicates on a 7500 Fast Real Time PCR System machine (Applied Biosystem, Foster City, CA, USA), according to manufacturer's instructions. Gene specific primers are: mouse Procollagen type I alpha 1 (Procol1A1) F: 5'-GAGCGGAGAGTACTGGATCG-3', R: 5'-GTTCGGGCTGATGTACCAGT-3'; mouse Procollagen type I alpha 2 (Procol 1A2) F: 5'-AGGCTGACACGAACTGAGGT-3', R: 5'-ATGCACATCAATGTGGAGGA-3'; mouse Procollagen type III alpha 1 (Procol3A1) F: 5'-AGGCTGAAGGAAACAGCAAA-3', R: 5'-TAGTCTCATTGCCTTGCGTG-3'; mouse Beta-Actin F: 5'-AGAGGGAAATCGTGCGTGAC-3', R: 5'-CAATAGTGATGACCTGGCCGT-3', and mouse Piezo 1, F: 5'-ACGCCAAGCTCATCTTCCT-3' , R: 5'-GTCCCTTTGACAGCAGCATC-3' (19). Relative procollagen gene expression between control and drained embryos at E 16.5 (24h PS), E17.5 (48h PS) and E18.5 (72h PS) was normalized to beta-actin (ΔCt), and control mouse larynges at E16.5 (ΔΔCt). Relative Piezo 1 gene expression between control and drained embryos was normalized to beta-actin (ΔCt) and control embryos collected at each time point (ΔΔCt). If undetected, a cycle number 40 was assigned to allow fold change calculation Data are presented as the average of two biological replicates (n=6) ± standard error of the mean. A Student's T test, ANOVA and a post hoc Tukey test were performed to calculate significance in gene expression levels. A p-value < 0.05 was considered significant.

Atomic force microscope sample collection and measurements

Dissected larynges from control and drained murine embryos at each time point (24h, 48h, and 72h) were embedded in a 4% w/v low-melt agarose (Dot Scientific, Burton, MI, USA). Fresh unfixed larynges were immediately cut into transversal sections using a vibratome, Leica VT 1000S, at frequency setting 8, speed setting 3, and thickness 150μm. Within 24 hours, transverse sections were placed on adhesive glass slides, submerged in PBS, and taken to the AFM at the University of Wisconsin Madison. The Bruker Catalyst Bio-AFM (Bruker Nano Surfaces, Santa Barbara, CA, USA) with spherical tip (r = 5 μm) silicon nitride cantilevers (Novascan Technologies, Boone, IA, USA), (nominal spring constant = 0.06 N/m, tip half angle 18°) were used to acquire ramp force curves. The cantilever was secured with a fluid tip holder, with all readings occurring in PBS. Cantilevers were calibrated on deflection sensitivity measurements on glass slides in PBS and harmonic oscillator thermal tunes in air. Single indentation force curves were taken in 3 spots per sample (20 readings per spot) in at least 3 VF samples for each condition (n=3). Probe indentation depth was 8 μm, which indented 5.3% of total tissue depth (well within the 10% maximum range).

Calculation of elastic modulus and statistical analysis

Curve slopes were calculated on the Hertzian indentation model using Nanoscope Analysis 1.5 Software (Bruker Nano Surfaces, Santa Barbara, CA, USA), with sample Poisson's ratio of 0.300. For each sample spot, baseline corrections were performed on curves and the elastic modulus measured from the curve slope. Data from each sample spot was pooled into data for each time point on experimental and control conditions. AFM reading errors report an elastic modulus of −1.000, these data were removed from the sample set. Outliers were identified and removed using the interquartile range filter, a standard filter for removing outliers on the basis of median rather than mean. Mean and standard deviation, and standard

error of the mean were calculated. The Fligner-Killeen test of homogeneity of variances was used to assess data variance. Due to unequal variance between data sets, Welch's ANOVA and a post hoc Games-Howell test were used to calculate significance, as they do not make assumptions about equal variance between groups. A p-value < 0.05 was considered significant.

Results

Drainage of amniotic fluid causes the delay in vocal fold recanalization and leads to intense epithelial remodeling

To investigate the role of amniotic load in EL separation, we first examined how VF morphology changed in both control and drained embryos 24, 48 and 72 hours post-surgery (PS). In the 24h PS control embryos, the VF were separated (Fig.2A), while in drained embryos the EL was still visible (Fig. 2B). Forty-eight hours PS the EL was completely disintegrated in both control and drained embryos (Fig. 2C, D). Notably, polyp-like structures with mesenchymal cores appeared cranially in control embryos (Fig. 2C) and more caudally, in the mid-membranous region, in the drained VF (Fig. 2D). In drained embryos, polyp-like structures were lined with a very thin one-layer epithelium (Fig. 2D). Seventy-two hours PS, polyp-like structures persisted in the VF regions in both control and drained embryos (Fig. 2E, F).

To confirm that epithelial cells underwent remodeling during recanalization we performed staining for p63, a marker of basal cells and cytokeratin (K) 8, a marker of suprabasal cells. In 24h PS control embryos, VF separated secondary to the continuous presence of amniotic fluid. The VF epithelium consisted of a well-defined p63+ K8- basal and p63- K8+ suprabasal cell layers (Fig. 3 A,B). In drained embryos, at the EL, the p63+ K8- basal cell layer was compact, however, at the same time the adhering suprabasal p63- K8+ layer lining the right and left VF started to detach (Fig. 3 C,D). This suggests that in drained embryos twenty-four hours PS, fluid began to build up in the larynx and acted on the EL recanalization. At forty-eight hours PS, in fully separated VF, the p63+ K8- basal layer appeared loosened, especially in the drained VF at the site of the polyp-like structure (Fig. 3 E–H). p63- K8+ suprabasal cells flattened and filled the space between the free-standing isolated p63+K8- basal cells protecting the lamina propria and VF epithelium became single-layered. Seventy-two hours PS, the VF epithelium was nearly restored with a two-layer p63+K8- and p63-K8+ arrangement, and re-established stratification in both control and especially drained VF (Fig. 3 I–L). To further investigate whether changes in amniotic fluid load also altered expression of typical airway epithelial markers, we stained for SOX2 and NKX2.1. While NKX2.1 expression was weak in both control and drained embryos at all selected time-points, we observed notable differences in SOX2 expression (Fig. 4 A–L). Twenty-four hours PS in both control and drained embryos, we detected strong anti-SOX2 staining in the VF epithelium (Fig. 4 A, C). However, 48h PS, SOX2 expression decreased in the mid-membranous region of drained VF in contrast to control VF (Fig. 4 E, G). Seventy-two hours PS SOX2 expression was re-established in the mid-membranous domain of the drained VF (Fig. 4 I, K), when the VF epithelium re-gained stratification. These data suggest that the decrease in amniotic fluid load delayed VF separation. Moreover, the

subsequent increase in mechanical load due to flow restoration caused forced EL disintegration impairing VF shape and triggering intense epithelial remodeling that affected expression of key VF epithelial genes, such as SOX2 and p63 and compromised the integrity of the basal cellular compartment.

Drainage and consequent flow restoration activate procollagen synthesis in VF fibroblasts with concomitant alteration in the stiffness of the lamina propria.

We next examined whether the changes in amniotic fluid load induced remodeling of the LP and modified production of extracellular proteins. First, we performed double immunofluorescent (IF) staining for Collagen 1 (Col 1), as a mesenchymal marker and K8, as an epithelial marker, to compare Col1 protein expression levels and distribution in the LP in control and drained embryos. Anti-K8 staining was performed to label the VF epithelium and show that Col1 expression was restricted to the mesenchymal compartment. In 24h PS control embryos, Col1 expression was found in the VF LP, particularly in the subglottic region (Fig. 5A). However, in drained embryos, anti-Col1 staining was reduced (Fig. 5B). At forty-eight and seventy-two hours PS, anti-Col 1 staining was detected in both control and drained VF (Fig. 5 C–F).

To further investigate collagen expression, we performed qPCR to measure mRNA levels. We compared transcript levels of Type I Procollagen alpha 1 (Procol1A1), Type I Procollagen alpha 2 (Procol1A2), and Type III Procollagen alpha 1 (Procol3A1) between control and drained embryos for each time point as well as changes in procollagen expression between time points. For this analysis, control embryos collected at E16.5 (24h PS) were used as controls for data normalization. Our findings show that in both control and drained embryos, Procol1A1 and Procol1A2 expression significantly increased with embryonic growth and maturation (Fig. 6 A, B). However, in control embryos, a substantial rise in Procol1A1 and Procol1A2 expression was detected between E16.5 (24h PS) and E17.5 (48h PS) with a tapering off expression of both procollagens at E18.5 (72h PS) (Fig.6 A, B). For drained embryos, procollagen transcript levels increased between E16.5 (24h PS) and E17.5 (48h PS) and were significantly upregulated between E17.5 (48h PS) to E18.5 (72h PS) as compared to controls (Fig. 6 A, B). A similar pattern was observed in Procol3A1 in both control and drained embryos (Fig. 6C). P-values showing significant changes in procollagen gene expression are summarized in Supplemental Tables 1 and 2.

To investigate whether drainage of amniotic fluid had an impact on elastic properties of the LP, we measured elastic moduli of the LP with AFM, in vibratome VF transversal sections. Our data show that in both control and drained conditions, the stiffness of the LP significantly increased between E16.5 (24h PS) and E17.5 (48h PS), with the LP from the drained VF being significantly softer than in controls at both time points (Fig 6D). However, while in controls there was no difference in the LP stiffness between E17.5 (48h PS) and E18.5 (72h PS) (Fig. 6D), in drained embryos the LP stiffness further increased, and the LP became stiffer than in control VF (Fig. 6D). P- values showing significant changes in the elastic modulus values of the LP are summarized in Supplemental Tables 3 and 4. These findings correlate with the pattern of procollagen expression in VF fibroblasts as described above (Fig. 6A–C). Collectively, these data suggest that changes in amniotic fluid load may

induce LP remodeling and activate of VF fibroblasts to produce extracellular matrix proteins that deposit in the LP and change elastic properties of the LP.

Alternations in amniotic fluid load activate Piezo 1-Yap signaling in the VF epithelium.

To elucidate how these events are regulated, we sought to determine the mechanosensitive Piezo1 –Yap signaling pathway activated by the changes in amniotic fluid load. First , we addressed the activity of Piezo1 which is a well described flow responsive ion channel (20,21). We evaluated Piezo 1 expression by immunohistochemistry and qPCR. Our data show that at twenty-four and forty-eight hours PS anti-Piezo1 staining was detected in drained VF epithelium and controls with the slightly higher intensity in drained samples (Fig. 7 A–D). Nevertheless, seventy-two hours PS, anti- Piezo1 staining intensity was similar to control samples (Fig. 7 E, F). For mRNA expression levels at 24h PS, in drained embryos, Piezo1 was significantly upregulated as compared to controls (Fig. 7G) and was downregulated at 48h PS to the transcript levels similar to control samples (Fig. 7G). At 72h PS, transcript levels of Piezo1 in drained VF significantly increased as compared to controls likely due to cellular changes associated with epithelial re-stratification (Fig. 7G). P- values showing significant alternations in Piezo 1 expression are summarized in Supplemental Tables 1 and 2.

Since Yap works as a downstream target of Piezo 1 signaling (22), we next evaluated pattern of Yap expression in control and drained embryos (Fig. 8). In control embryos, anti-Yap staining was mainly located in the cytoplasm and was observed in the VF epithelium (Fig. 8 A,B, E,F K and L). The intensity of Yap expression was highest at E16.5 (24h PS) and gradually decreased in more advanced embryonic stages, E17.5 (48h PS) and E18.5 (72h PS). In drained embryos 24h PS, anti-Yap staining was cytoplasmic, and it was detected in the VF epithelium, particularly in the supraglottic region (Fig. 8 C, D). Forty eight hours PS, after complete VF separation, Yap was translocated into the nucleus mainly in epithelial cells that lined the polyp-like structure (Fig. 8 G–I). A few Yap+ nuclei were also detected in the adjacent LP. 72h PS, epithelial anti-Yap staining became cytoplasmic again and its intensity started to decrease (Fig. 8 M, N).

Collectively, we show that the decrease in amniotic fluid load and the onset of the fluid re-accumulation in the larynx 24h PS was capable of activating Piezo 1 ion channels in the VF epithelium which then triggered Yap translocation into the nucleus (48h PS) and activated signaling pathways involved in remodeling of the VF epithelium and the LP.

Discussion

Recently published genetic studies provided insight into how genes and signaling factors control differentiation of VF epithelial and mesenchymal progenitors during EL recanalization (13,16,17), but very little is known about external mechanical forces and their role in this process. The EL is a temporal structure that needs to be resorbed in the developing larynx for normal VF functioning in voicing, breathing and swallowing (23). In a mouse, breathing movements and amniotic fluid inhalation are first observed at E14.5 (18), which coincides with EL recanalization (9,10). Synchrony between EL recanalization and fetal breathing allows amniotic fluid to pass through the larynx down into the lungs where it

acts on differentiation of distal alveoli (3). Open airways are also critical for removal of lung secretions produced by alveolar cells (24). In a sonographic examination of a human fetus the marked polyhydramnious and echogenic lungs often indicate congenital upper airway obstructive lesions such as laryngeal webs, atresia or tracheoesophageal fistula (23).

In this study, we focused on the epigenetic force-induced mechanisms of EL recanalization that were disrupted by the drainage of amniotic fluid. Our findings show that amniotic fluid assists in EL recanalization and guarantees gradual VF separation in a time specific manner to minimize traumatic effects. However, alternations in mechanical load due to drained and restored flow causes delayed and rapid EL recanalization which resulted in VF tissue deformation that promoted load-related remodeling of the VF epithelium and LP likely mediated by Piezo1-Yap signaling pathway in the VF epithelium.

First, we examined the effect of amniotic fluid on EL disintegration. Twenty-four hours PS in drained animals, the VF collapsed, whereby postponing recanalization. Nevertheless, forty-eight hours PS, the VF completely separated in drained embryos. This relatively rapid VF separation could be caused by the re-accumulation of fluid flowing through the larynx. These findings correlate with previous investigations. In a mouse fetal rupture model, histological analyses of the perforated sites of the amnion after drainage of amniotic fluid at E15.5 show that the perforation diameter significantly decreased at 24h PS, and the puncture was closed after 48 and 72 hours PS allowing amniotic fluid to build up in the sac (25). We postulate in this investigation that during EL recanalization, rapid re-accumulation of amniotic fluid increased the mechanical load and the EL finally disintegrated, effecting VF shape and remodeling.

Next, we showed that pressure generated structural reorganization of the epithelium mainly affected the compactness of the p63+ basal cell layer and SOX2 expression. Forty-eight hours PS, after a complete EL recanalization, SOX2 expression markedly decreased and p63+K8- basal cells segregated allowing suprabasal cells to spread between basal cells and maintain barrier function. This reorganization resulted in a temporal loss of the stratified phenotype. The VF epithelium regenerated, and re-established stratification seventy-two hours PS, when basal p63+K8- progenitors and SOX2+ cells re-appeared in the VF epithelium. Along with epithelial remodeling, we observed adaptive changes in the LP suggesting that VF epithelial cells closely interact with VF fibroblasts and extracellular matrix (ECM). We saw no difference in procollagen expression at twenty-four and forty-eight hours PS between drained and control samples, when amniotic fluid started to build up in the larynx. However, we measured enhanced production of procollagens in VF fibroblasts in drained embryos seventy-two hours PS (Supplemental Tables 1 and 2), as a response to complete flow restoration. Similar physiological responses to changes in mechanical load were reported in *in vitro* cell cultures of adult VF fibroblasts (26) confirming that mechanical forces are capable to modulate VF fibroblast functions in ECM production and degradation (27–30). These findings support the notion that ECM composition responds specifically to changes in load, which is critical for connective tissue homeostasis and maintenance of tissue mechanics (31,32).

In order to evaluate VF tissue mechanics during EL recanalization and changes in the LP elasticity due to drainage of amniotic fluid we utilized AFM (33). We completed AFM measurements on unfixed vibratome VF sections (preserved nearly all the properties of living tissue and enabled us to study VF biological samples in their natural microenvironment). We measured a decrease in stiffness of the LP in drained VF 24 and 48h PS as compared to controls and a significant increase in elastic modulus values in the VF LP of drained samples 72h PS, which correlates with procollagen upregulation in VF fibroblasts of drained embryos. Enhanced production and deposition of ECM components, by connective tissue, is a common feature of load induced hypertrophy which may lead, under pathological conditions, to tissue fibrosis and permanent changes to tissue mechanics (32).

Understanding reciprocal interactions between the ECM and epithelial and/or mesenchymal cells that modify ECM composition and architecture still remains a challenge in molecular cell biology. In this study we linked, for the first time, a stretch-sensitive ion channel Piezo 1 with the process of the EL recanalization and structural changes in the VF epithelium and the LP. We show that alternations in the mechanical load were capable of activating Piezo 1 expression in VF epithelial cells 24h PS (Fig. 9). Nevertheless, at 48h PS Piezo 1 expression was considerably decreased corresponding with epithelial transformation and basal cell layer remodeling. The elevated transcript levels of Piezo1 detected prior to VF epithelial and ECM remodeling, suggest that Piezo 1 can participate in stimulation of signaling pathways involved in epithelial regeneration and activation of VF fibroblasts in the LP. One of the possible mechanisms is via modulation of the nuclear localization of the transcription coactivator Yap which is a downstream target of Piezo 1 (22). We have shown here that 48h PS Yap translocated into the nucleus where it likely regulated expression of target genes involved in re-stratification of the VF epithelium and adaptive changes in the LP. These results are in accordance with recent studies have shown that Yap-Taz signaling pathway is capable of stimulating epithelial repair along with ECM remodeling including collagen 1 deposition via matrix-mediated integrin signaling (34). Besides Piezo 1 signaling, several other growth factor and transcription factor signaling pathways have been identified to work downstream of mechanical forces in development and repair in mice. These include several members of the Transforming Growth Factor (TGF) superfamily, including TGFbeta and Bone Morphogenetic Proteins (BMPs) (4,35). Further experiments are needed to investigate their role in stimulation of VF repair and regeneration in response to the mechanical force during VF embryogenesis.

Conclusion

Our observations lay the foundation for further functional experiments to uncover the role of mechanical load in VF development, homeostasis and tissue repair. Understanding the links between the mechanical and biological parameters is key to gaining insights into disease pathophysiology and mechanisms of congenital laryngeal disorders as well as mechanisms of VF tissue remodeling in response to mechanotransduction.

Supplementary Material

Refer to Web version on PubMed Central for supplementary material.

Acknowledgements

This work was supported by grants NIH NIDCD R01 DC004336 and R01 DC012773. We gratefully acknowledge Sierra Raglin for her expert assistance with the paraffin sample preparation for this study.

References

1. Goddard LM, Duchemin A, Ramalingan H, Zhou B, Vermot J, Kahn ML, et al. A Article Hemodynamic Forces Sculpt Developing Heart Valves through a KLF2-WNT9B Paracrine Signaling Axis. Dev Cell. 2017;43:274–89. [PubMed: 29056552]
2. Ranade SS, Qiu Z, Woo SH, Hur SS, Murthy SE, Cahalan SM, et al. Piezo1, a mechanically activated ion channel, is required for vascular development in mice. Proc Natl Acad Sci U S A. 2014 7 15;111(28):10347–52. [PubMed: 24958852]
3. Li J, Wang Z, Chu Q, Jiang K, Li J, Tang N. The Strength of Mechanical Forces Determines the Differentiation of Alveolar Epithelial Cells. Dev Cell. 2018 2 5;44(3):297–312.e5. [PubMed: 29408236]
4. Subramanian A, Kanzaki LF, Galloway JL, Schilling TF. Mechanical force regulates tendon extracellular matrix organization and tenocyte morphogenesis through TGFbeta signaling. 2018; Available from: 10.7554/eLife.38069.001
5. Behrndt M, Salbreux G, Campinho P, Hauschild R, Oswald F, Roensch J, et al. Forces Driving Epithelial Spreading in Zebrafish Gastrulation. Science (80-). 2012;338(October):257–60.
6. Culver JC, Dickinson ME. The effects of hemodynamic force on embryonic development. Microcirculation. 2010;17(3):164–78. [PubMed: 20374481]
7. Hamada H Role of physical forces in embryonic development. Semin Cell Dev Biol [Internet]. 2015;47–48:88–91. Available from: 10.1016/j.semcdb.2015.10.011
8. Keller R, Shook D, Skoglund P. The forces that shape embryos: Physical aspects of convergent extension by cell intercalation Vol. 5, Physical Biology. Institute of Physics Publishing; 2008.
9. Henick DH. Three-Dimensional Analysis Of Murine Laryngeal Development. Ann Otol Rhinol Laryngol Suppl. 1993;159:3–24. [PubMed: 8457128]
10. Lungova V, Verheyden JM, Herriges J, Sun X, Thibeault SL. Ontogeny of the mouse vocal fold epithelium. Dev Biol. 2015;399(2).
11. Sanudo J, Domenech-Mateu JM. The laryngeal primordium and epithelial lamina. A new interpretation. J Anat. 1990;171:207–22. [PubMed: 2081706]
12. Zaw-Tun HA, Burdi AR. Reexamination of the origin and early development of the human larynx. Acta Anat (Basel). 1985;122(3):163–84. [PubMed: 4013651]
13. Lungova V, Verheyden JM, Sun X, Thibeault SL. β-catenin signaling is essential for mammalian larynx recanalization and the establishment of vocal fold progenitor cells. Dev. 2018;145(4).
14. Wyatt ME, Hartley BEJ. Laryngotracheal reconstruction in congenital laryngeal webs and atresias. Otolaryngol Neck Surg. 2005;132(2):232–8.
15. Hartnick CJ, Cotton RT. Congenital Laryngeal Anomalies Laryngeal Atresia , Stenosis , Webs , and Clefts. Otolaryngol Clin North Am −. 2000;33(6).
16. Ebert B, Sidman J, Morrell N, Roby BB. Congenital and iatrogenic laryngeal and vocal abnormalities in patients with 22q11.2 deletion. Int J Pediatr Otorhinolaryngol. 2018;109(March):17–20. [PubMed: 29728175]
17. Huh SH, Ornitz DM. β-Catenin deficiency causes DiGeorge syndrome-like phenotypes through regulation of Tbx1. Development. 2010;137(7):1137–47. [PubMed: 20215350]
18. Abadie V, Champagnat J, Fortin G. Branchiomotor activities in mouse embryo. Neuroreport. 2000;11(1):141–5. [PubMed: 10683846]
19. Yamazaki K, Fukata H, Adachi T, Tainaka H, Kohda M, Yamazaki M, et al. Association of increased type I collagen expression and relative stromal overgrowth in mouse epididymis neonatally exposed to diethylstilbestrol. Mol Reprod Dev. 2005 11;72(3):291–8. [PubMed: 16086434]

20. Ellefsen K, Chang A, Nourse J, Holt J, Arulmoli J, Mekhdjian A, et al. Piezo1 calcium flickers localize to hotspots of cellular traction forces. Piezo1 calcium flickers localize to hotspots Cell Tract forces. 2018;294611.
21. Zhang T, Chi S, Jiang F, Zhao Q, Xiao B. A protein interaction mechanism for suppressing the mechanosensitive Piezo channels. Nat Commun. 2017 12 1;8(1).
22. Pathak MM, Nourse JL, Tran T, Hwe J, Arulmoli J, Le DTT, et al. Stretch-activated ion channel Piezo1 directs lineage choice in human neural stem cells. Proc Natl Acad Sci U S A. 2014 11 11;111(45):16148–53. [PubMed: 25349416]
23. Liberty G, Boldes R, Shen O, Shaul C, Cohen SM, Yagel S. The fetal larynx and pharynx: Structure and development on two- and three-dimensional ultrasound. Ultrasound Obstet Gynecol. 2013;42(2):140–8. [PubMed: 23239522]
24. Condon JC, Jeyasuria P, Faust JM, Mendelson CR. Surfactant protein secreted by the maturing mouse fetal lung acts as a hormone that signals the initiation of parturition [Internet]. 2004 Available from: www.pnas.orgcgidoi10.1073pnas.0401124101
25. Mogami H, Hari Kishore A, Akgul Y, Word RA. Healing of Preterm Ruptured Fetal Membranes. Sci Rep. 2017 12 1;7(1).
26. Li NY, Heris HK, Mongeau L. Current Understanding and Future Directions for Vocal Fold Mechanobiology. J Cytol Mol Biol. 2013;1(1):9.
27. Wolchok JC, Brokopp C, Underwood CJ, Tresco PA. The effect of bioreactor induced vibrational stimulation on extracellular matrix production from human derived fibroblasts. Biomaterials. 2009 1;30(3):327–35. [PubMed: 18937972]
28. Gaston J, Quinchia Rios B, Bartlett R, Berchtold C, Thibeault SL. The response of vocal fold fibroblasts and mesenchymal stromal cells to vibration. PLoS One. 2012 2 16;7(2).
29. Kirsch A, Hortobagyi D, Stachl T, Karbiener M, Grossmann T, Gerstenberger C, et al. Development and validation of a novel phonomimetic bioreactor. PLoS One. 2019 3 1;14(3).
30. Webb K, Hitchcock RW, Smeal RM, Li W, Gray SD, Tresco PA. Cyclic strain increases fibroblast proliferation, matrix accumulation, and elastic modulus of fibroblast-seeded polyurethane constructs. J Biomech. 2006;39(6):1136–44. [PubMed: 16256125]
31. Chiquet M, Renedo AS, Huber F, Fluck M. How do fibroblasts translate mechanical signals into changes in extracellular matrix production? Vol. 22, Matrix Biology. 2003.
32. Viji Babu PK, Rianna C, Mirastschijski U, Radmacher M. Nano-mechanical mapping of interdependent cell and ECM mechanics by AFM force spectroscopy. Sci Rep. 2019 12 1;9(1).
33. Babu PKV, Radmacher M. Mechanics of brain tissues studied by atomic force microscopy: A perspective Vol. 13, Frontiers in Neuroscience. Frontiers Media S.A; 2019.
34. Yui S, Azzolin L, Maimets M, Pedersen MT, Fordham RP, Hansen SL, et al. YAP/TAZ-Dependent Reprogramming of Colonic Epithelium Links ECM Remodeling to Tissue Regeneration. Cell Stem Cell. 2018 1 4;22(1):35–49.e7. [PubMed: 29249464]
35. Gumucio JP, Sugg KB, Mendias CL. TGF-β Superfamily Signaling in Muscle and Tendon Adaptation to Resistance Exercise. Exerc Sport Sci Rev. 2015 Apr 11;43(2):93–9. [PubMed: 25607281]

Highlights

- Drainage of amniotic fluid delays vocal fold separation
- Decreased and consequent flow restoration induces remodeling of the epithelium.
- Changes in mechanical load alter the stiffness of the lamina propria.
- Load-related remodeling of the mucosa is likely regulated by Piezo 1-Yap signaling.

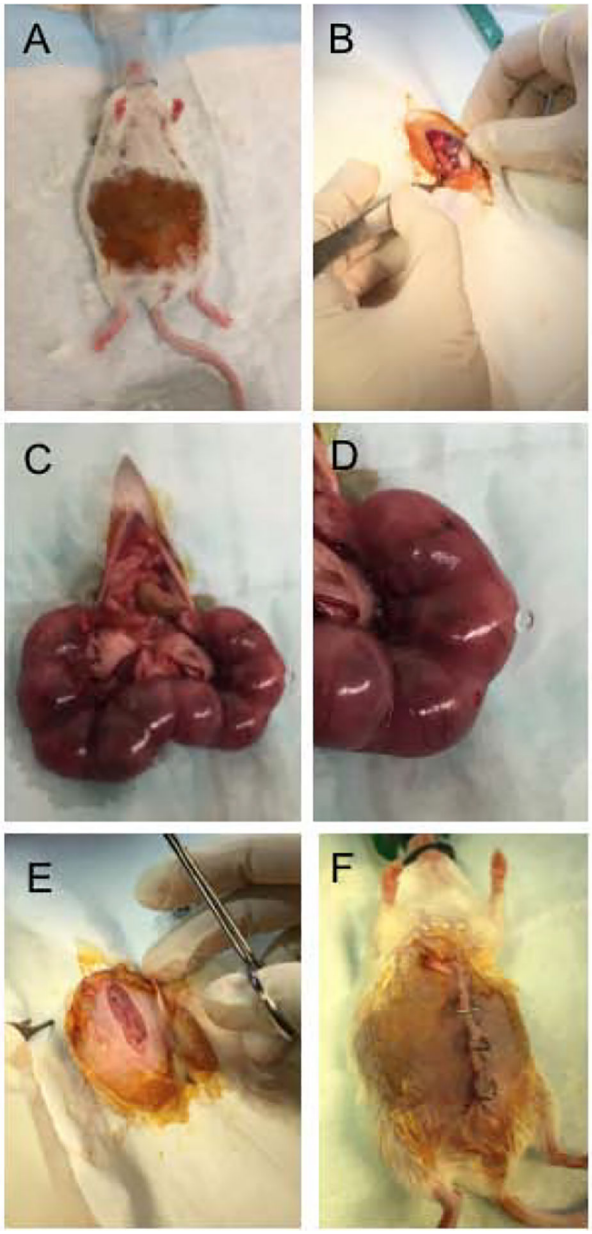

Figure 1: Drainage of amniotic fluid surgery.

Pregnant females at day 15.5 gestation underwent surgery under isoflurane anesthesia (A). The peritoneum was opened (B), and embryos were removed (C). One third of the total number of embryos underwent a puncture of the amniotic sac with a 25G needle (D). Remaining embryos were left as controls to prevent spontaneous abortion or preterm labor. After the perforation, embryos were returned to their initial position. The peritoneal cavity was flushed with saline and closed with sutures (E), the skin was closed with clips (F). Pregnant females were then sacrificed at E16.5, E17.5, and E18.5 (24, 48 and 72 hours post-surgery).

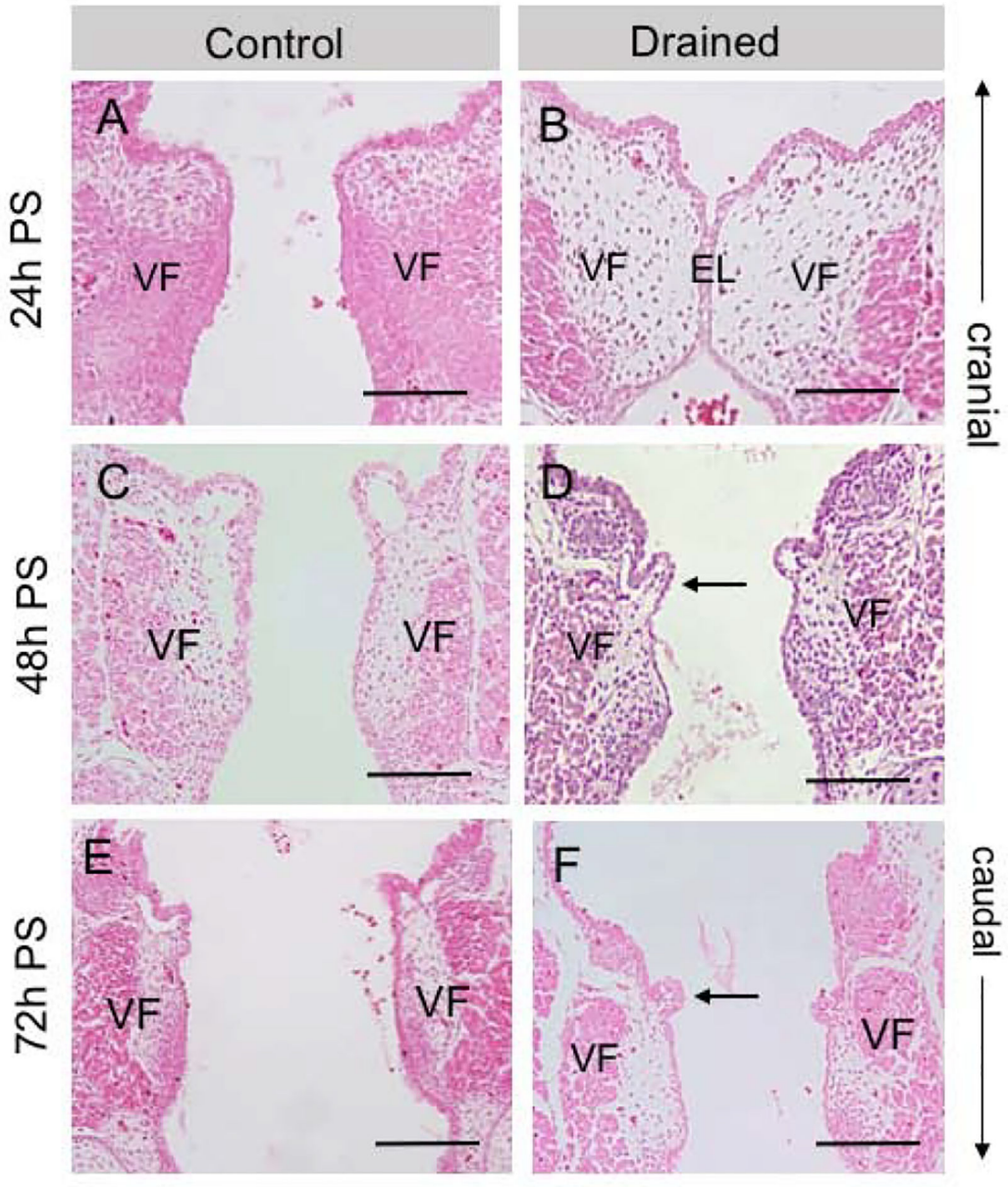

Figure 2: Characterization of VF morphology.

(A, B) Hematoxylin-eosin staining demonstrating a completely disintegrated EL in control embryos (A) and a visible EL in drained VF 24h PS (B). (C, D) Hematoxylin-eosin staining showing completely resorbed EL 48h PS in both control (C) and drained embryos (D). In drained VF, polyp-like structures appear in the mid-membranous region on the right and left VF (black arrow). These structures are lined with a very thin one-layer VF epithelium. (E, F). Hematoxylin-eosin staining demonstrating separated VF in control (E) and drained samples (F). Polyp-like structures persist in the mid-membranous VF region (black arrow). Scale bar = 100μm. Abbreviations: EL, epithelial lamina; h, hour; PS, post-surgery; VF, vocal fold.

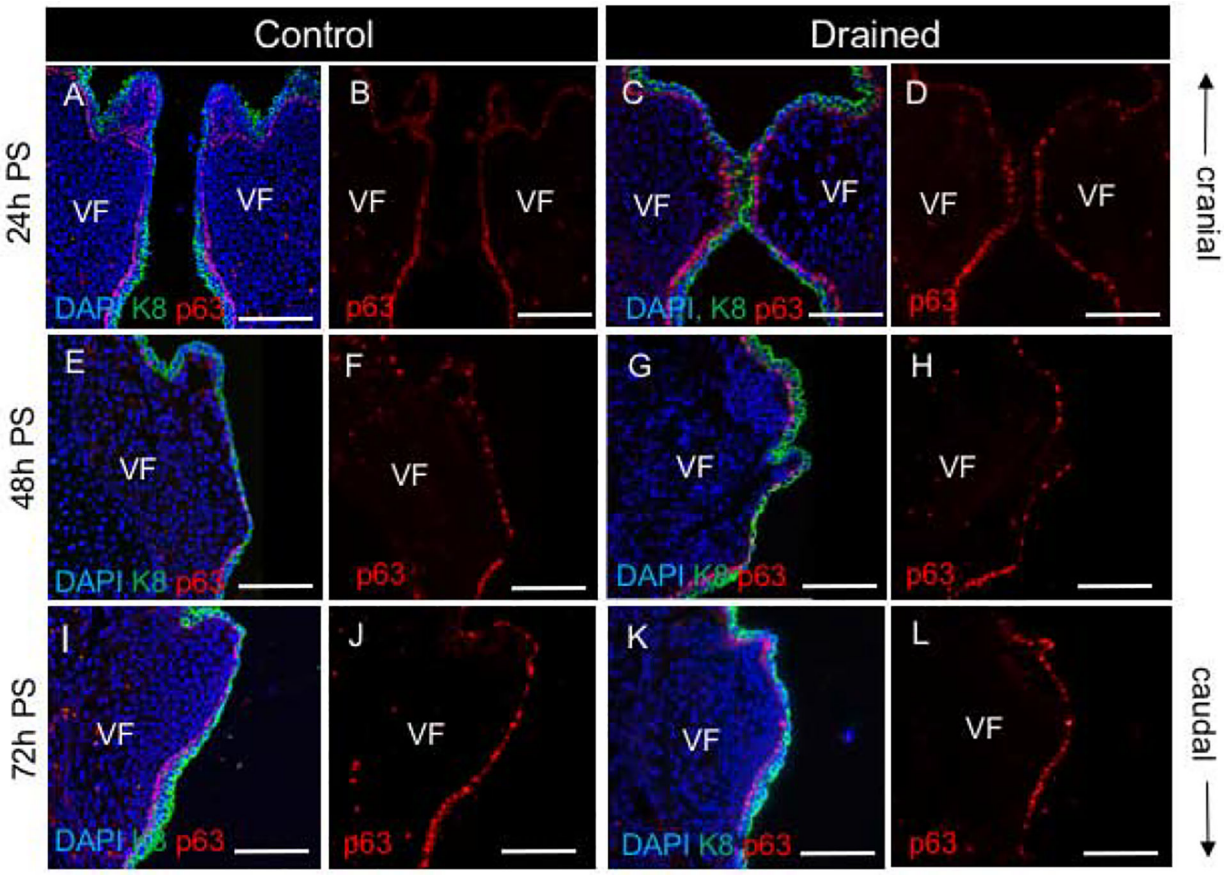

Figure 3: VF epithelial remodeling during EL recanalization.

(A, C) Double staining for p63 (red) and Cytokeratin K8 (green) in control (A) and drained embryos (C) showing epithelial remodeling 24h PS. (B, D) A single channel p63 expression in control (B) and drained embryos (D). In control embryos, the VF are separated, and each VF is lined with p63+K8- basal and p63-K8+ suprabasal cell layers. In drained embryos, the p63+K8- basal layer is compact, while adherent p63-K8+ suprabasal cell layers start to detach. (E, G) Double staining for p63 (red) and Cytokeratin K8 (green) in control (E) and drained embryos (G) showing epithelial remodeling 48h PS. (F, H) A single channel p63 expression in control (F) and drained embryos (H). In drained embryos, at the site of the polyp-like structures, the basal p63+K8- cell layer almost disappears. P63-K8+ suprabasal cells spread between segregated basal cells. The VF epithelium temporarily loses stratified phenotype (white arrow). (I, K) Double staining for p63 (red) and Cytokeratin K8 (green) in control (I) and drained embryos (K) showing re-established stratification in the VF epithelium in control and drained vocal folds at 72h PS. (J,L) A single channel p63 expression in control (J) and drained embryos (L). Scale bar = 100μm. Abbreviations: h, hour; PS, post-surgery; VF, vocal fold.

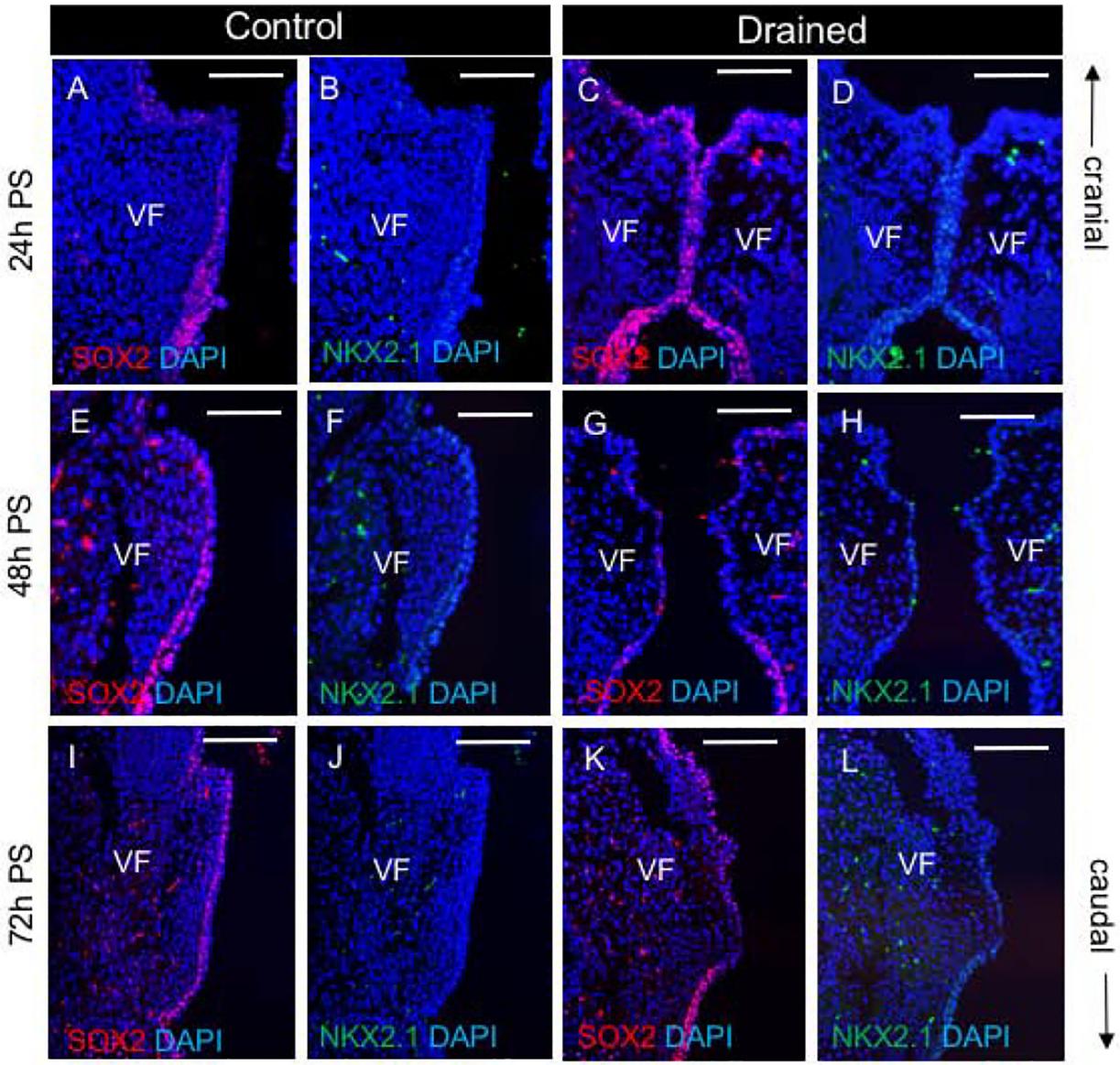

Figure 4: Changes in SOX2 and NKX2.1 expression during EL recanalization.

(A-D) Double staining for SOX2(red) and NKX2.1 (green) in control (A, B) and drained embryos (C, D). (E-H) Double staining for SOX2 (red) and NKX2.1 (green) in control (E, F)) and drained embryos (G, H)) showing downregulation of SOX2 in drained embryos 48h PS. (I-L) Double staining for SOX2 (red) and NKX2.1 (green) in control (I,J) and drained embryos (K,L) showing re-established SOX2 expression in drained vocal folds at 72h PS. Scale bar = 100μm. Abbreviations: h, hour; PS, post-surgery; VF, vocal fold.

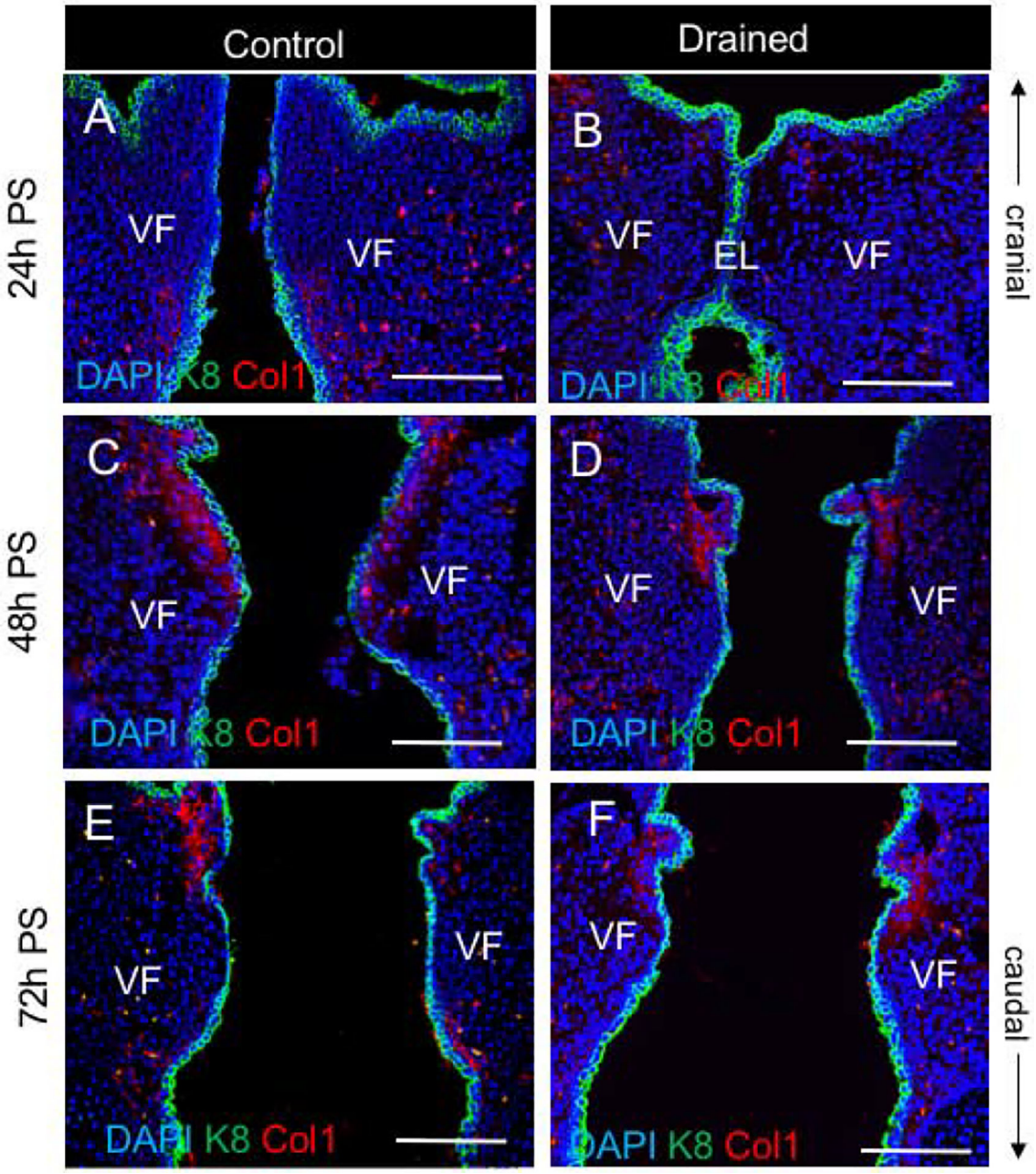

Figure 5: Deposition of Collagen1 in the lamina propria during the EL recanalization.

(A, B) Double staining for Col1 (red) and Cytokeratin K8 (green) in control (A) and drained embryos (B) 24h PS. In control VF, Col1 is detected particularly in the subglottic VF region. In drained VF, Col1 staining is reduced. (C - F) Double staining for Col1 (red) and Cytokeratin K8 (green) in control (C, E) and drained embryos (D, F) 48h and 72h PS, respectively. Collagen 1 expression was detected in both control and drained VF. Scale bar = 100μm. Abbreviations: EL, epithelial lamina; h, hour; PS, post-surgery; VF, vocal fold.

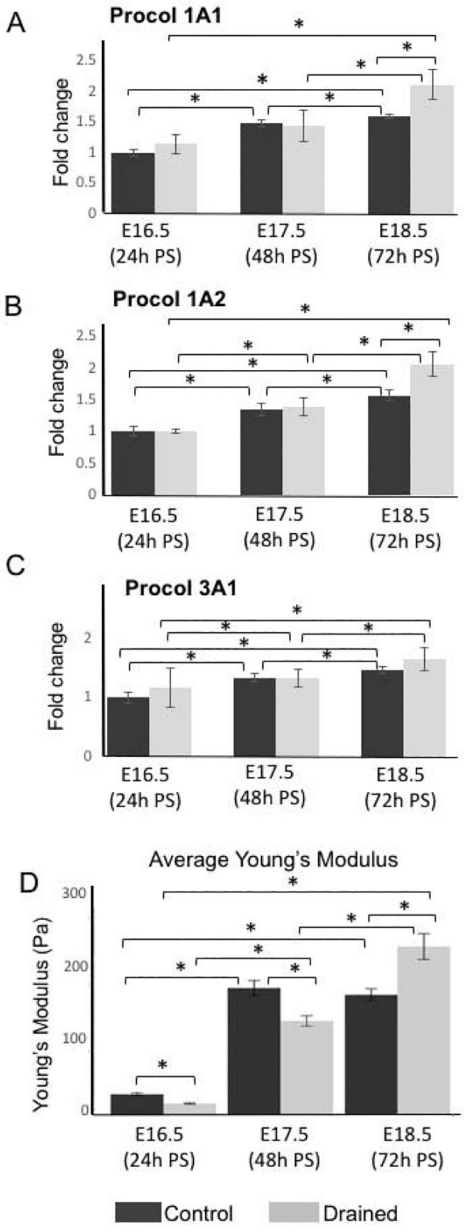

Figure 6: Changes in the transcript levels of procollagens during the epithelial recanalization, measurement of the elastic modulus.

(A-C) Transcript levels of Procol1A1, Procol1A2 and Procol3A1 in control and drained vocal folds 24h, 48h and 72h PS. For qPCR analysis, control embryos collected at E16.5 (24h PS) were used as controls for ΔΔCT data normalization. Data are presented as the average of two biological replicates (n=6) ± standard error of the mean, as three mouse larynges were pulled together for one biological replicate to maximize RNA yield. A Student's T-test, ANOVA and post hoc Tukey test were performed to calculate significance in the gene expression levels between control and drained embryos at each time point and between time points. A p-value < 0.05 (*) was considered significant. (D) Measurements of the elastic modulus in control and drained VF. 24h and 48h PS in drained samples the lamina propia was significantly softer than in control VF. However, at 72h PS the stiffness of

the lamina propria in drained samples significantly increased, which correlates with the increased expression of collagens in the lamina propria. A Welch ANOVA and a post hoc Games-Howell test were used to calculate significance, as they do not make assumptions about equal variance between groups. A p-value < 0.05 (*) was considered significant

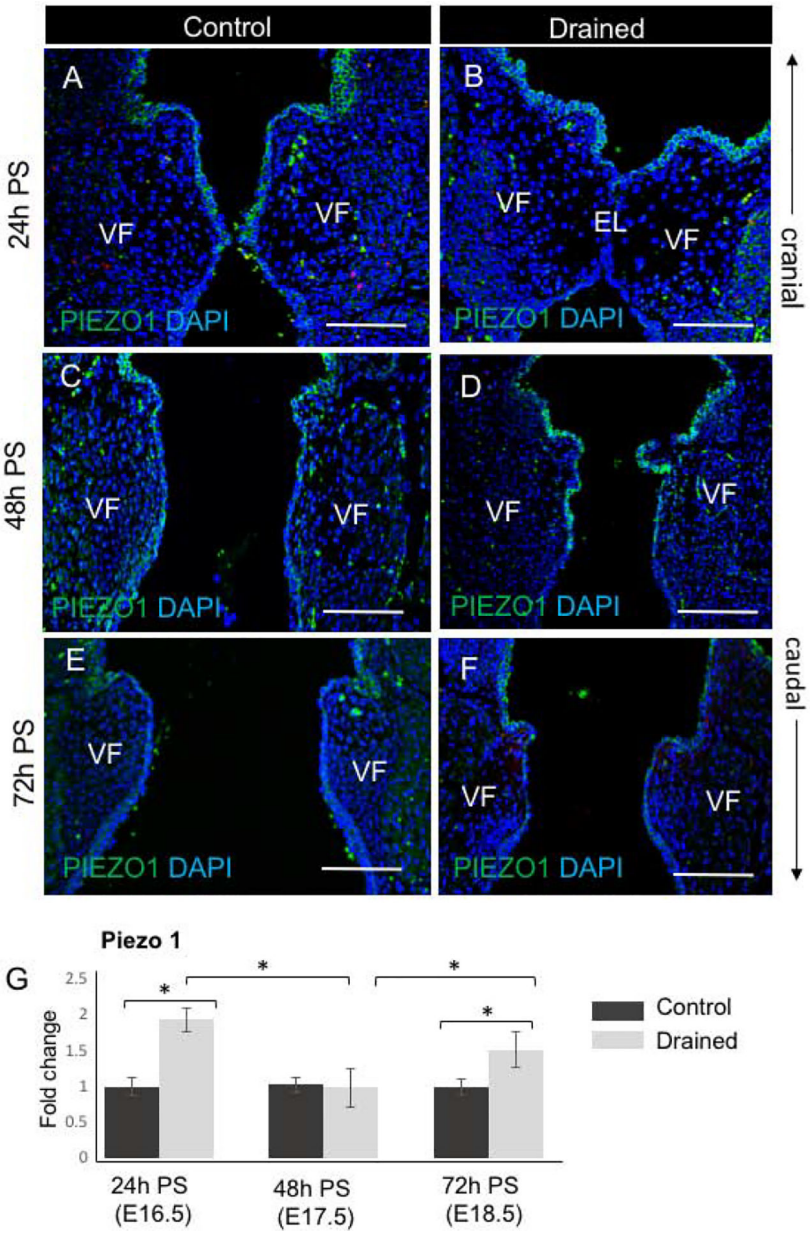

Figure 7: Piezo 1 expression during the EL recanalization.

(A - F) Characterization of Piezo 1 expression (in green) in VF epithelial cells during the EL recanalization in control VF (A, C, E) and drained VF (B, D, F) 24h, 48h and 72h PS, respectively. Strong Piezo 1 staining was detected particularly in drained embryos 24h and 48h PS. Scale bar = 100μm. Abbreviations: EL, epithelial lamina; h, hour; PS, post-surgery; VF, vocal fold. (G) mRNA expression levels of Piezo 1 in control and drained VF 24h, 48h, and 72h PS. For qPCR analysis, control embryos collected at each time point were used as controls for ΔΔCT data normalization. Data are presented as the average of two biological replicates (n=6) ± standard error of the mean, as three mouse larynges were combined for one biological replicate to maximize RNA yield. A Student's T test, ANOVA and a post hoc Tukey test were performed to calculate significance in the gene expression levels between

control and drained embryos at each time point. A p-value < 0.05 (*) was considered significant.

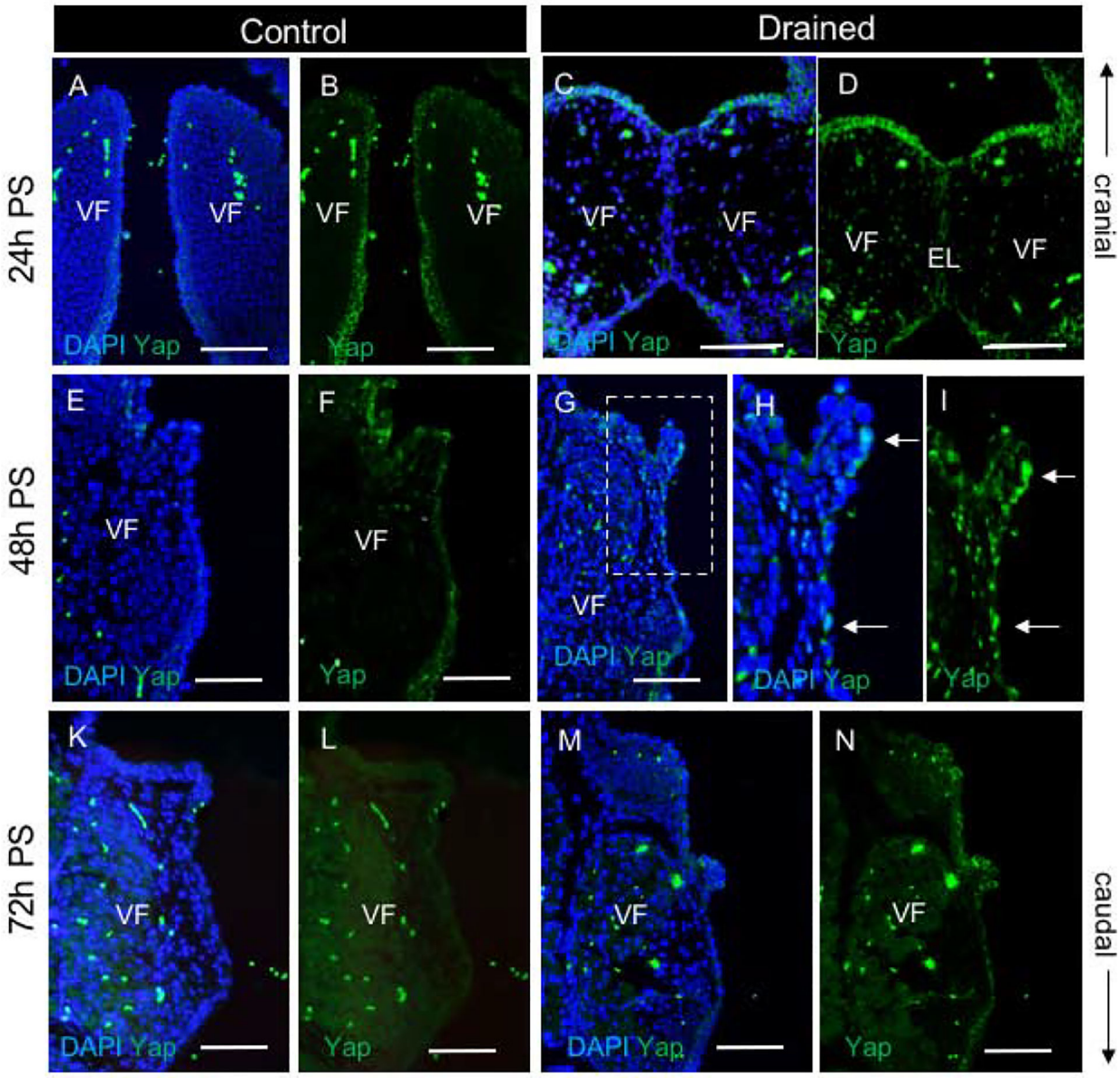

Figure 8: Yap expression during EL recanalization.

(A-D) Staining for Yap (green) in control (A, B) and drained embryos (C, D) showing cytoplasmic localization of Yap in VF epithelial cells. A single channel Yap expression in control (B) and drained embryos (D). (E-I) Staining for Yap (green) in control (E, F) and drained embryos (G-I) showing translocation of Yap into the nucleus in VF epithelium lining the polyp-like structure 48h PS (white solid arrows). A bracketed region in the panel of G is magnified in the panels of H and I. A single channel Yap expression in control (F) and drained embryos (I). (K-N) Staining for Yap (green) in control (K, L) and drained embryos (M, N) showing weak cytoplasmic Yap expression in the VF epithelium in control and drained vocal folds at 72h PS. A single channel Yap expression in control (L) and drained embryos (N). Scale bar = 100μm. Abbreviations: EL, epithelial lamina; h, hour; PS, post-surgery; VF, vocal fold.

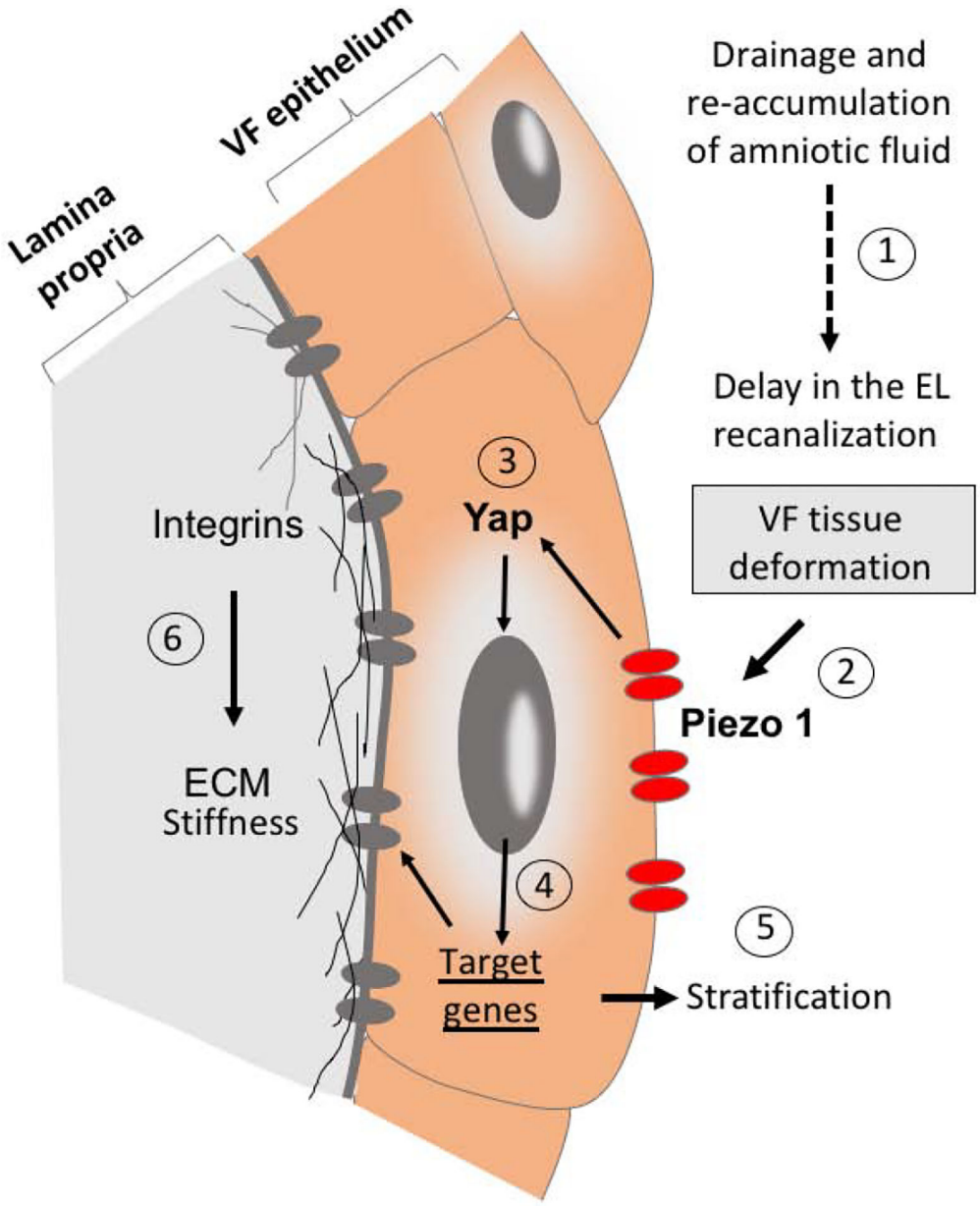

Figure 9: Schematic illustration of the proposed mechanism of Piezo1 – Yap regulation of epithelial and mesenchymal remodeling.

(1) Drainage and re-accumulation of amniotic fluid in the laryngeal region cause delayed and rapid EL recanalization which altered VF shape and led to VF tissue deformation. (2) Overall VF tissue deformation then activated Piezo 1 sensory channels in the plasma membrane of VF epithelial cells, which triggered Yap translocation into the nucleus (3) and promoted expression of target genes (4) involved in epithelial stratification (5) and extracellular matrix remodeling in the lamina propria (6). Abbreviation: ECM, extracellular matrix; EL, epithelial lamina; VF, vocal folds.